Monolayer doping of germanium with arsenic: a new chemical route to achieve optimal dopant activation.

Noel Kennedy,[1] Shane Garvey,[1,2] Barbara Maccioni[2], Luke Eaton,[1,2] Michael Nolan[2], Ray Duffy,[2] Fintan Meaney,[2] Mary Kennedy,[3] Justin D. Holmes,[1] and Brenda Long.[1]*

[1] School of Chemistry & AMBER Centre, University College Cork, Cork, T12 YN60, Ireland.

[2] Tyndall National Institute, Lee Maltings, University College Cork, Cork, T12 R5CP, Ireland.

[3]Scientific Process Development Services, Tarbert, Kerry, Ireland

Abstract

Reported here is a new chemical route for the wet chemical functionalization of germanium (Ge), whereby arsanilic acid is covalently bound to a chlorine (Cl) terminated surface. This new route is used to deliver high concentrations of arsenic (As) dopants to Ge, via monolayer doping (MLD). Doping, or the introduction of Group III or Group V impurity atoms into the crystal lattice of Group IV semiconductors, is essential to allow control over the electronic properties of the material to enable transistor devices to be switched on and off. MLD is a diffusion-based method for the introduction of these impurity atoms via surface bound molecules which offers a non destructive alternative to ion implantation, the current industry doping standard, making it suitable for sub-10 nm structures. Ge, given its higher carrier mobilities, is a leading candidate to replace Si as the channel material in future devices. Combining the new chemical route with the existing MLD process yields active carrier concentrations of dopants ($>1 \times 10^{19}$ atoms/cm^3), that rival those of ion implantation. It is shown that the dose of dopant delivered to Ge is also controllable by changing the size of the precursor molecule. X-ray photoelectron spectroscopy (XPS) data and density functional theory (DFT) calculations support the formation of a covalent bond between the arsanilic acid and the Cl terminated Ge surface. Atomic force microscopy (AFM) indicates that the integrity of the surface is maintained throughout the chemical procedure and electrochemical capacitance voltage (ECV) data shows carrier concentrations of 1.9×10^{19} atoms/cm^3 corroborated by sheet resistance measurements.

Introduction

The dimensions of CMOS components, *i.e.* transistors, have decreased over the decades from being in the order of micro to nano-metres in accordance with the prediction of Moore's law.[1, 2] The aggressive scaling down of transistors has placed demands on the engineering required to keep up with this, calling for dramatic alterations to the architectures of the devices as well as the processes such as doping, deposition, and lithography.[3, 4]

Ge is the most likely material to be used, together with Si, to improve the performance of future transistors. It offers the advantages of increased (2.7 time) electron and (4 time) hole mobility over Si[5] and their similarity (both are Group 4 elements) means it can be seamlessly integrated into a CMOS fabrication process utilising the same infrastructure. Alternative channel materials, such as III-Vs, would require new costly infrastructure and are considerably more expensive to produce and process than Ge.

One of the most fundamental processes in transistor fabrication is the introduction of impurity atoms into the semiconductor to allow them to function as switching devices. Beam-line based ion implantation has long been the industry leading method of carrying out semiconductor doping.[6] This is a process which involves bombarding the structure with dopant ions, a side effect of which is crystal damage. Larger and planar structures can be annealed at high temperature to restore the crystal integrity. However, in dimensions approaching sub-10 nm, ion implantation induces damage that cannot be reversed by annealing.[7] Furthermore, the directional nature of beam-line implantation has significant issues when applying the technique to tightly pitched arrays of nanostructures. The nanostructures in these arrays create shadows which can lead to non-conformality, giving high variability in device characteristics, and poor dopant incorporation into the sidewalls.[8, 9] To address the issue of crystal damage, implantation development has moved from room temperature towards high temperature conditions known as hot implantation.[10-12] However, these do not address the issue of shadowing and non-conformality for arrays of nanostructures. An alternative to ion implantation, plasma doping, has been developed to address problems with directionality and crystal damage, but still has conformality issues.[13, 14] Nonetheless, with further device scaling, novel methods will be required for these advanced doping applications where ideally the solution will be capable of producing minimal crystal damage and a conformal doping without the directionality constraints.

Monolayer doping (MLD), first reported in 2008,[15] is a diffusion based, and therefore non-destructive method, for introducing dopants and has the potential to deliver conformal doping of nanostructures without issues of directionality. MLD is a deposition doping technique in which a controllable dose is provided through a self-limiting surface adsorbed monolayer of organic molecules containing the dopant atom. The self-limiting nature of monolayer formation allows for a controlled dose which is defined by the size of the molecular precursor. The dopant atoms are transported into the target structure via diffusion during an annealing step which causes the adsorbed molecule to decompose releasing the dopant. While, MLD has been well studied and used to dope Si,[16-23] silicon-germanium alloys,[24] and III-V's[25, 26] it has been less studied for Ge doping.[27-29]

Finding new methods to non-destructively dope Ge to the required dopant concentration is imperative given the use of Ge not only as the channel material in FETs, but also in other devices, which requires doping concentrations typically on the order of 1×10^{19} atoms/cm^3. The application of MLD to Ge doping with As is challenging but is worth investigating due to the controllable As diffusion and high solubility in Ge, while the diffusion of both boron and phosphorus (via MLD using conventional annealing) is too slow to achieve any meaningful doping.[30] Sgarbossa *et al* showed useful results for antimony (Sb) doping achieving a concentration of ~3×10^{18} atoms/cm^3 using conventional annealing.[28, 31] However when laser annealing was employed record levels of Sb (~1×10^{20} atoms/cm^3) activation were achieved and successful P (~2×10^{19} atoms/cm^3) incorporation was also produced. However, despite these high doping concentrations, we have to remember that laser annealing involves melting the surface of the semiconductor and is therefore not suitable for processing nanostructures as they would lose their structural integrity.

As-MLD in germanium has not been studied to the same extent as other n-type dopants, likely due to the toxicity of the traditional molecular precursors. Previous work in the area of As-MLD also required synthesis of As precursors as there was no commercially available molecule which can undergo the hydrogermylation reaction. This reaction had to this point, been the most consistent means of producing a chemically bound, self-limiting, monolayer for MLD.[32] However, large amounts of toxic waste are generated, which is dangerous and expensive to dispose of. Also, the synthesised precursors were prone to oxidation therefore extremely difficult to work with.[27, 33-36]

There is huge interest in chemical functionalisation of semiconductors. By modifying the surface of Si or Ge it is possible to control its functionality with applications that extend well beyond MLD such as photovoltaics, [37] electroactivity [38] and biointerfacing [39] for example. Loscutoff and Bent comprehensively reviewed the topic of organic functionalization of Ge in 2006.[40] They acknowledged that wet chemical functionalization methods on Ge were limited, with only three viable wet chemistry methods 1) hydrogermylation 2) thiolation and 3) Grignard reaction.

With the above discussion in mind, the present study, describes a novel route for chemical functionalisation of Ge and represents a significant advancement in the field as it is transferrable to a broad range of materials. This new route, adapted to permit controlled doping of Ge substrates with As, is summarised in **Figure 1** Furthermore, we also demonstrate, by comparing with existing data, that the As dose can be finely controlled by controlling the size of the adsorbed molecular precursor, while first principles simulations elucidate the binding mode of the precursor to the Ge substrate. Finally, we demonstrate for the first time on Ge that the maximum limits of electrically active arsenic has been achieved by MLD making it a truly viable alternative to other more destructive, less conformal, techniques, such as ion implantation.

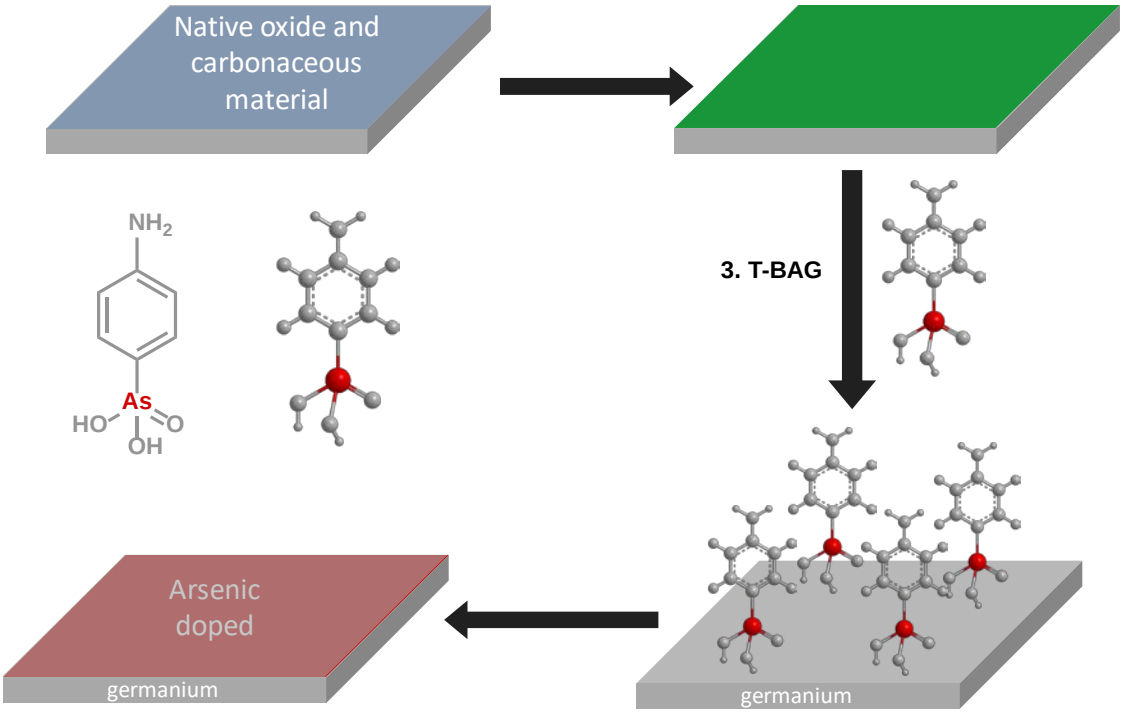

Figure 1: *Illustration of the novel chemical functionalisation procedure using arsanilic acid on a Cl terminated Ge surface.*

Experimental

All chemicals were purchased from Sigma-Aldrich and used as received. Planar p-type Ge wafers (100) with intrinsic carrier concentrations of ~ 1×10^{16} atoms/cm^3 were diced into 1 cm^2 samples for MLD processing.

Carbon contamination and debris from the dicing process was cleaned by sonicating in acetone for 2 minutes followed by a dip in 2-propanol (IPA) with drying under a stream of nitrogen.

Chlorine termination was produced by placing the Ge samples into a solution of 10% HCl for 10 minutes. Once a hydrophilic-like Cl terminated Ge surface was achieved a subsequent nitrogen dry was carried out in an effort to remove any traces of the HCl solution. Samples were then placed in a solution of 0.007 g / 50 ml arsanilic acid in suitable solvent which after testing was chosen to be dichloromethane (≥99.9%). This solution was left to evaporate and once done, a physisorbed arsanilic acid residue remained on the samples. Chemical binding of the arsanilic acid monolayer was carried out through the Tethering By AGgregation (T-BAG) method which required annealing at 140 °C in a vacuum oven for a period of 10 hours. [41] Once this chemisorption step was complete a final clean was carried out to remove the excess physisorbed material. A 2-minute sonication in methanol followed by a further dip in methanol and nitrogen drying was used to clean this physisorbed material.

A sputtered SiO_2 capping layer was used to promote dopant diffusion into the semiconductor substrate during annealing. Capping layers were deposited prior to annealing which was done in a12 rapid thermal annealing (RTA) system at temperatures from 400-700 °C and times varying between 1-100 seconds. The capping layers were then removed using a dilute solution of buffered oxide etch (BOE). This process was refined to ensure minimal surface damage to both planar and non-planar samples.

Electrochemical capacitance voltage (ECV) profiling was carried out to determine active carrier concentration with depth in the MLD doped samples. A CVP 21 profiler was used with a 0.1 M Tiron solution as the etchant solution. Etch steps of 5/10/20/40 nm were chosen depending on profile depth and to minimize measurement error a relaxation period of 30 seconds was implemented between etch and measurement steps. Error in concentration values was below 5 % for all levels greater than 1×10^{18} atoms/cm^3 and only slightly increased above this value for lower concentrations. Water contact angle measurements were taken with an Ossila contact angle goniometer and utilised as an indication of surface conditions. Atomic force microscopy was conducted

under ambient conditions in tapping/non-contact mode using Veeco Multi-mode V microscope. Scan area for all measurements was 3 x 3 µm.

X-ray photoelectron spectroscopy measurements were taken with a Kratos axis ultra-spectrometer using a mono Al K 1486.58 eV, 150 W x-ray gun. For Survey spectra a pass energy of 160 eV, step of 1 eV, dwell of 50 ms, and 3 sweeps were used. Core spectra were taken with a pass energy of 20 eV, step of 1 eV, dwell of 50 ms, and 2-10 sweeps. Data processing was carried out on CasaXPS software with calibration using the C 1s line at 284.8 eV as charge reference.

A Lucas labs 302 manual four-point probe tool was utilised for Rs measurements along with a Keithley power supply.

The adsorption mechanism of arsanilic acid on a model Cl-terminated Ge surface, which prevents reconstruction of the Ge (100) surface and is consistent with Cl-termination of Ge used in the experiments, has been studied using density functional theory (DFT). In particular our investigation focuses on determining the adsorption of arsanilic acid on Cl-terminated Ge (100) surface. All DFT calculations of geometry and electronic structure have been performed within DFT using the generalized gradient approximation (GGA) as implemented in the Vienna Ab Initio Software Package (VASP.5.4.1) program.[42, 43] The core-valance electron interactions are described by potentials constructed with the projector augmented-wave (PAW) method[44]; the following valance electron configurations are used Ge $4s^2$ and $4p^2$, As $4s^2$ and $4p^3$, C $2s^2$ and $2p^4$, O $2s^2$ and $2p^2$, N $2s^2$ and $2p^3$ and H 1s. The exchange-correlation energy was evaluated with the PBE approximation to the exchange-correlation functional.[45] In all calculations, the cutoff energy is 420 eV, the energy is converged when the difference between successive steps is less than 10^{-4} eV and the forces are converged when they are below 0.02 eV/Å. Given the supercell dimensions, we use Γ-point sampling for the Brillouin zone integrations.

The Ge (100) surface is described by a 3D periodic surface slab composed of 4 Ge-atomic layers with a 2x2 surface supercell expansion; this gives eight atoms in the outermost layer of the surface. The two faces of the Ge surface are separated by a vacuum region of 40 Å and the top and bottom layers are passivated with one Cl per surface Ge atom. Ionic relaxations are performed with the atoms belonging to the two bottom Ge-layers constrained while the others atoms were allowed to relax with no symmetry constraints.

To investigate the interaction of arsanilic acid on the Cl-terminated Ge (100) surface we have calculated the adsorption energies (E_{ads}) using the following expression:

$$E_{ads} = E_{molecule\text{-}Ge+Cl} + nE_{HCl} - E_{Ge+Cl} - E_{molecule}$$

where E_{Ge+Cl} and $E_{molecule\text{-}Ge+Cl}$ are the total energies of the Cl-termianted Ge surface and with the arsanilic acid adsorbed. *n* is the number of HCl removed from the system during adsorption, E_{HCl} is the energy of a gas phase HCl molecule and $E_{molecule}$ is the energy of the isolated arsanilic acid, all computed using the same technical parameters and set-up of the previous systems. Given the magnitude of the adsoprtion energies found, we do not include van der Waals interactions in the adsoprtion calculations, as these will not lead to any significant change in the adsorption energies.

Results and Discussion

Kary et al,[46] outlined in their patent from 1957, a solution based method of forming arsono-siloxane molecules which involved the reaction of a halosilane with an arsonic acid through a nucleophilic substitution reaction. Nucleophilic substitution is a commonly used strategy in organic chemistry. It involves the attack of a nucleophile to a target carbon molecule which contains a suitable leaving group with an inversion of the stereochemistry. In theory this stereochemistry inversion would not be possible on crystalline substrates. Interestingly, Si has shown an alternative trend to carbon when undergoing these nucleophilic substitution reactions with no inversion in stereochemistry.[47] The T-BAG method of chemically binding a monolayer to a crystalline substrate has previously been demonstrated as a successful method of attaching phosphonic acid monolayers to Si oxide by Chabal *et al*.[41] In this paper we have employed this nucleophilic substitution strategy, combined with the T-BAG method as a novel method of Ge functionalization.

Figure 1 illustrates the reaction procedure for arsanilic acid with the Ge surface. The first steps involved degreasing the sample by sonicating in acetone to remove carbonaceous material and its termination using chlorine (Cl). Cl termination of Ge has been well described in literature with reports showing that a dip in a dilute solution of hydrochloric acid serves to both remove the native oxide and Cl-terminate the surface with minimal roughening of the Ge substrate.[48] Water contact angle (WCA) measurements were carried out to determine the

change in the hydrophobicity of the surface as an indication of the Cl-termination. WCA values of as-received Ge were ~ 60° with this value decreasing to ~ 35-40°, as expected, as Cl terminated surfaces are known to be hydrophilic.

The functionalisation procedure outlined in the experimental section was carried out on these Cl-terminated samples with the aim of chemically binding a monolayer of arsanilic acid to the Ge surface. One of the key findings from previous T-BAG literature is that the presence of humidity prevents the formation of a covalent bond. In order to minimise humidity, this reaction was carried out in a vacuum oven. After the vacuum oven anneal, the Ge substrate was sonicated in methanol to remove any physisorbed species. A control sample which had undergone annealing in a standard oven and the same post-anneal cleaning procedure was also prepared. An XPS study of these samples, as well as an as-received and Cl terminated Ge wafer was carried out. **Figure 2** shows the survey spectra XPS data, highlighting the region around 1326 eV where the As 2p peak can be seen. This data clearly shows that the As 2p peak is only present on the sample (pink line) which has undergone the vacuum oven annealing step. This finding agrees with the previous T-BAG literature in showing that vacuum is essential for the covalent binding of the monolayer. The absence of an As 2p peak on the sample that was annealed in a standard oven would suggest that the sonication of the sample post-anneal in methanol is effective for the removal of non-covalently bound (physisorbed) arsanilic acid molecules. Core level spectra of As 2p and As 3d peaks from the As MLD with vacuum sample are shown in Figure **S1**. Quantification of the As on Ge is not currently possible via XPS as the As 3d peak overlaps with a Ge plasmon while the As 2p has no known relative sensitivity factor (R.S.F).

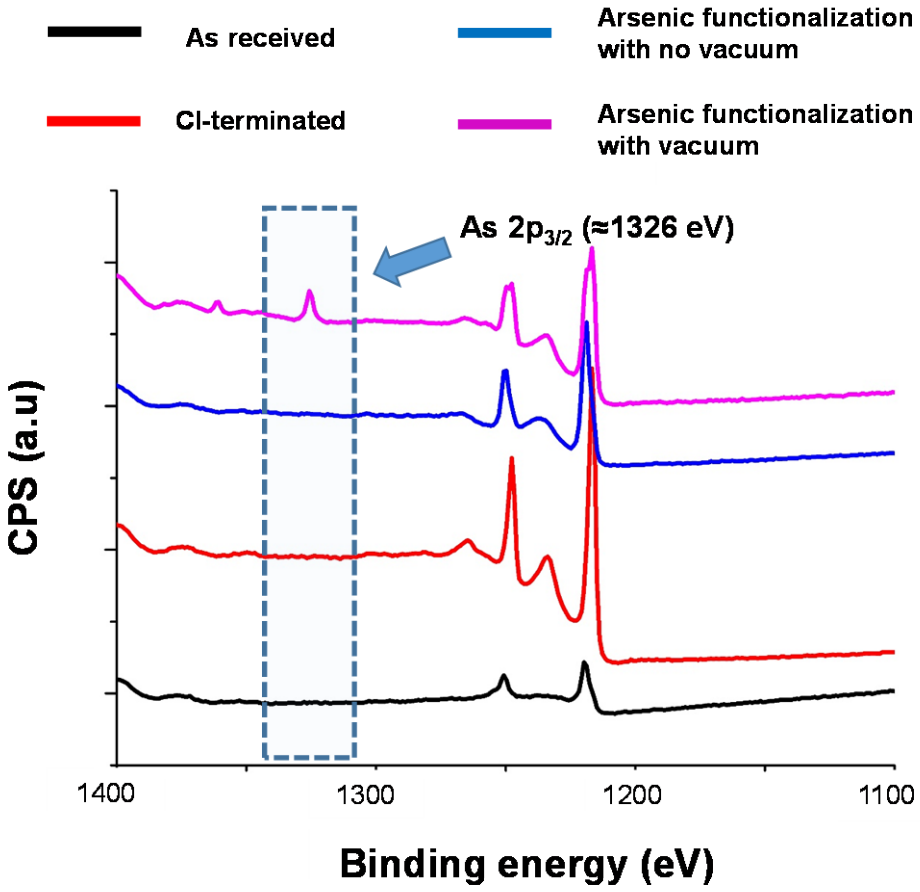

Figure 2: *XPS survey spectra of as received and Cl terminated Ge and arsanilic acid functionalised Ge, annealed at 140 °C for 10 hours, with and without a vacuum.*

Analysis of the core level Ge 3d signal analysed by XPS is shown in **Figure 3** and **Figure S2**. After HCl treatment of the Ge samples it can been seen that there is a significant reduction in the oxide component of the Ge 3d signal at ~33 eV. The sample which has undergone functionalization and annealed in the absence of a vacuum, has returned to a condition similar to the as-received Ge. Under ambient conditions the re-oxidation process would have been much slower, however the elevated temperature combined with humidity, in the absence of a vacuum, promotes this oxidation. The sample which has undergone functionalization with a vacuum oven anneal shows a small growth in the peak at ~33eV. It is noted that after 1 week (t = 168 hrs) the contribution from this peak remains the same indicating that the monolayer functionalized sample is stable.

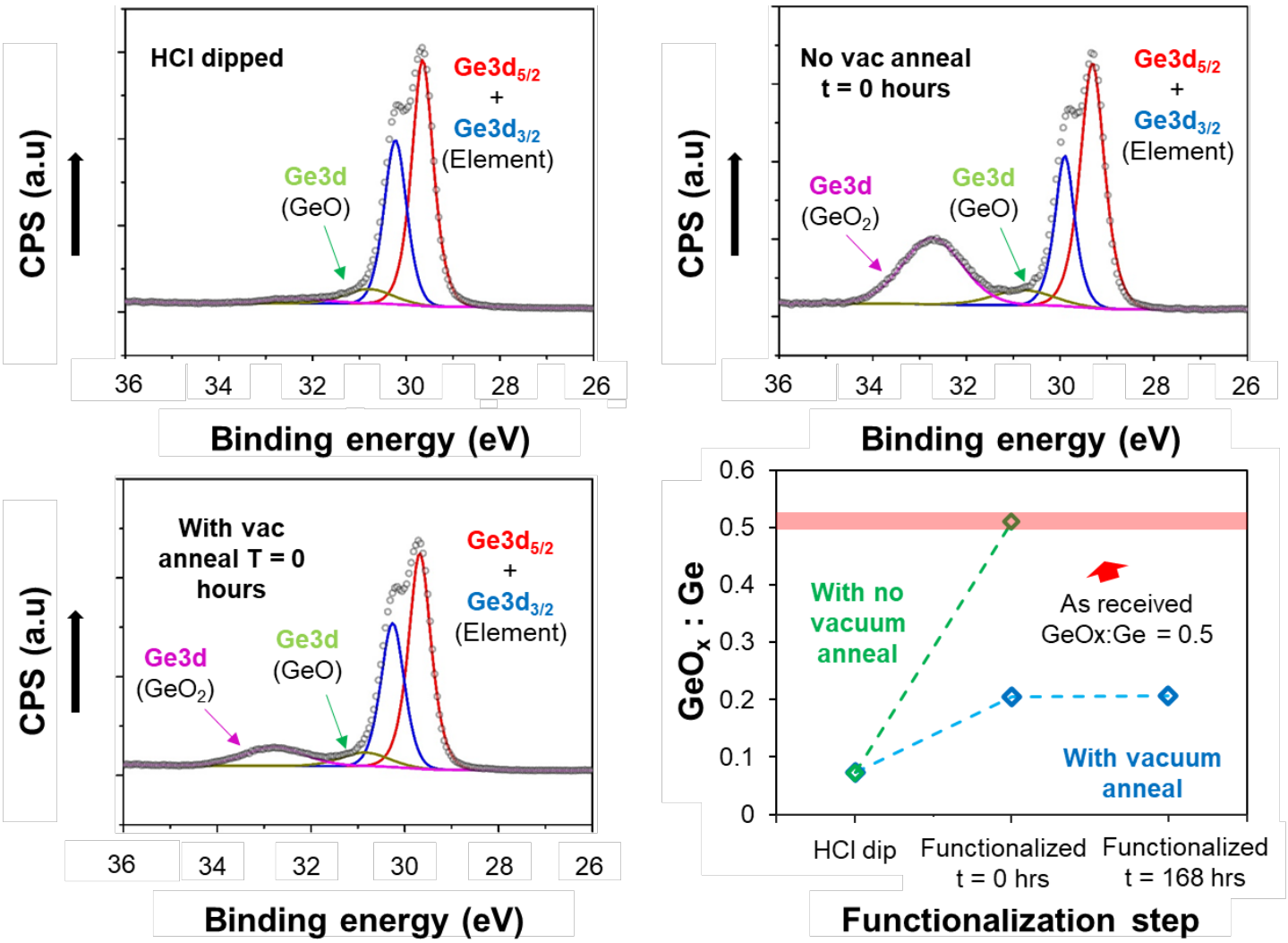

Figure 3: *XPS analysis of the Ge 3d peak for (a) Cl terminated (b) Arsanilic acid functionalised annealed in the absence of vacuum and (c) Arsanilic acid functionalised annealed in the presence of vacuum and (d). Analysis of GeOx:Ge over time for the arsanilic acid functionalised samples with and without a vacuum anneal. t= 0 hours represents samples analysed immediately after completion of the monolayer grafting process while t= 168 hours represents a sample which has undergone the grafting process and has subsequently been stored for 168 hours in ambient conditions before analysis.*

We use first principles density functional theory (DFT) to model the adsorption of the arsanilic acid molecule to a model Ge substrate to determine the preferred binding mode of the molecule. **Figure 4** shows a schematic of the adsorption process and identifies three likely binding modes, two through the acid group, using two oxygen sites (removing two surface Cl atoms) or one oxygen site (removing one surface Cl atom) and the third through the amino group, removing one surface Cl atom.

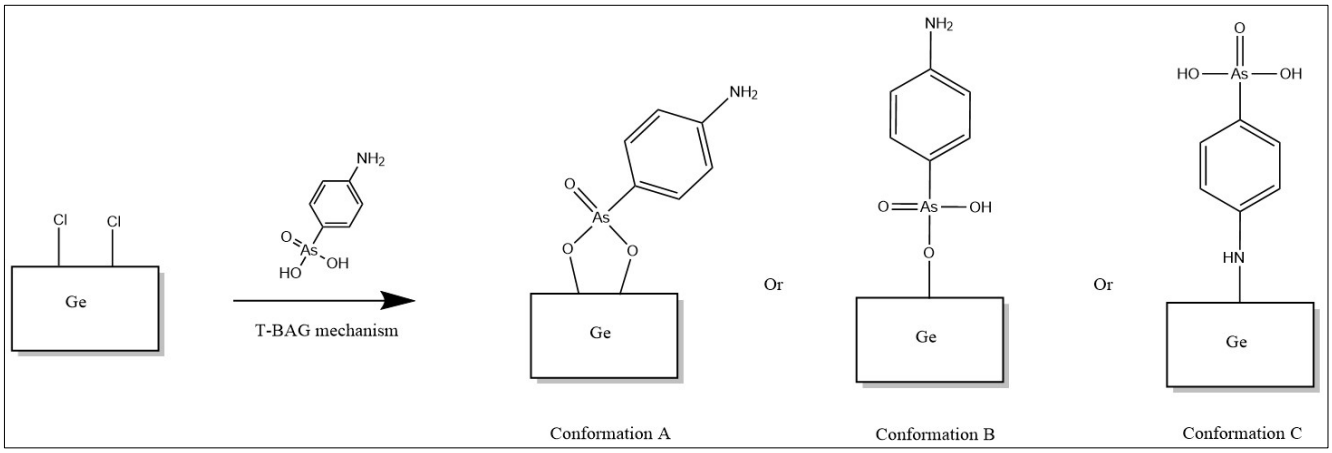

Figure 4: *Possible surface binding conformations of the As-acid molecule to the Ge surface*

Figure 5 shows the atomic structure of the Cl-terminated Ge(100) surface and relaxed adsorption structures for the three adsoprtion modes described above. The computed adsorption energies are -4.97 eV for Configuration A, -5.70 eV for Configuration B and -3.66 eV for Configuration C. Therefore the arsanilic acid molecule can in principle adsorb at Ge (100) in all three configurations, with loss of HCl. However, we note that configuration B, in which one oxygen atom from the acid group initially binds to one Ge atom in the (100) surface, relaxes so that adsorption takes place through two oxygen atoms in the molecule. These oxygen atoms each coordinate to different surface Ge atom (inset of Figure 5(c)). In the other adsorption modes the interaction is through two oxygen atoms in the acid group (Configuration A) or the nitrogen atom in the amino group (Configuration C). In addition, in configuration B, the phenyl ring tilts relative to the Ge surface.

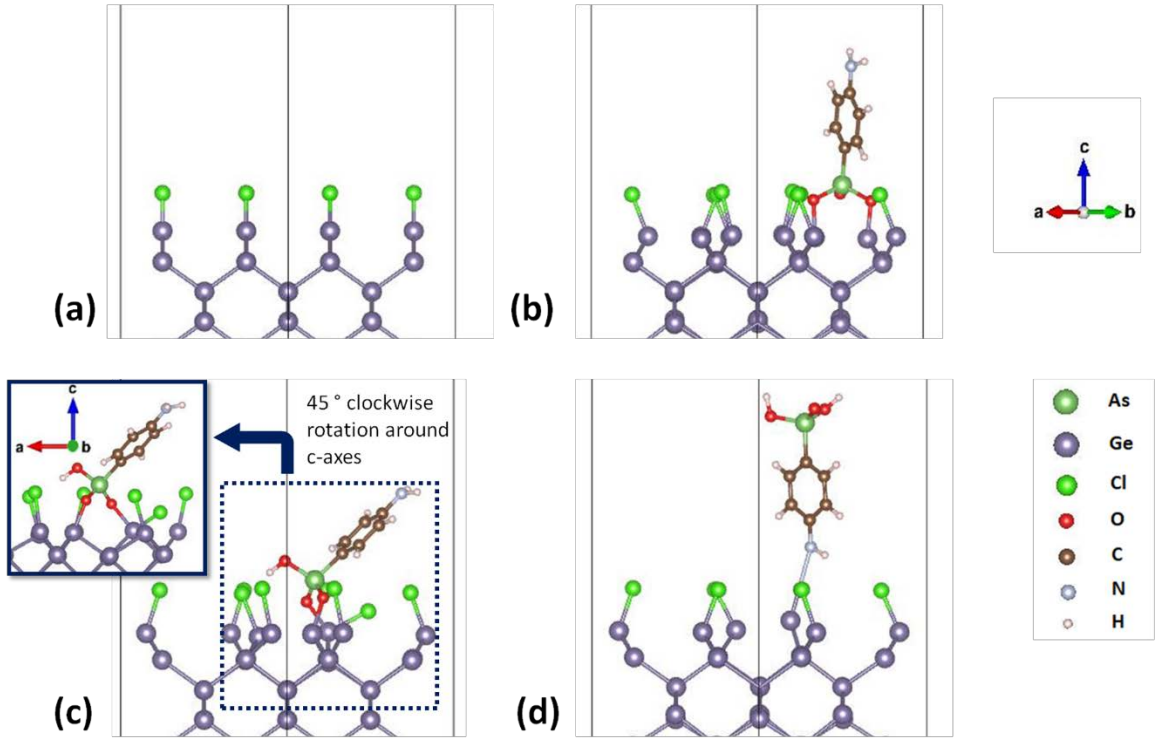

Figure 5: *Atomic structure of* ***(a):*** *Cl-terminated Ge (100) surface,* ***(b):*** *relaxed adsorption structure of arsanilic acid in Configuration A,* ***(c):*** *relaxed adsorption structure of arsanilic acid in Configuration B and* ***(d):*** *relaxed adsorption structure of arsanilic acid in Configuration C.* In panel **(c)** we also show a rotated view so that the As-O-Ge bonds can be seen.

In Configuration B, one Ge atom maintains a Ge-Cl bond, with a Ge-O distance of 1.93 Å. The second Ge-O distance is 1.92 Å and the As-O distances are 1.74 Å. Finally, the distance from As to the hydroxyl oxygen that does not bind to the surface, As-OH, is 1.75 Å. During the relaxation the As-O distances in the molecule increase by 0.09 Å and 0.06 Å for those oxygen binding to Ge and decrease by 0.05 Å for the As-OH bond. This change in metal-oxygen distances is consistent with the strong adsorption energy.

In Configuration A, the Ge-O distance involving the initially unprotonated oxygen is 1.86 Å , while for the other oxygen it is 2.01 Å. The O-As distances are 1.65 Å for oxygen that forms the double bond with As and 1.80 Å for the oxygen binding to the surface. Finally, in the least stable configuration, Configuration C, the Ge-N distance is 3.71 Å and the interaction is clearly weaker and we do not expect this binding mode to be of importance in the MLD process.

Finally, we note that after adsorption and ionic relaxation, surface Ge and surface terminating Cl atoms are distorted away from their initial positions in the Cl-terminated Ge (100) surface. For example we see a clear tilting of the surface terminating Cl atoms.

As-MLD functionalized samples were capped with 50 nm of sputtered SiO_2. It has previously been shown that the deposition of a capping layer is essential in the MLD process to optimise the diffusion of the dopant atoms from the surface into the bulk of the target semiconductor.[16, 34] Following capping, the samples were annealed using an RTA system and prepared for characterization by removing the cap using a dilute BOE solution. AFM imaging of samples after each processing step, shown in **Figure 6**, was carried out to monitor the surface roughness. Initial starting Ge (Fig 6. A) shows a high-quality surface with a roughness value of 0.26 nm. A slight increase in surface roughness is noted after the MLD processing steps with a final roughness of 0.55 nm. This increase in surface roughness is considered suitable for transfer to nanostructured Ge as it remains within ± 0.3 nm of the initial starting value. If roughness values were to increase significantly after MLD processing on blanket samples one would envisage, that given the dimensions of current and future nanostructured Ge, there would be the potential for structure damage and even complete structure loss.

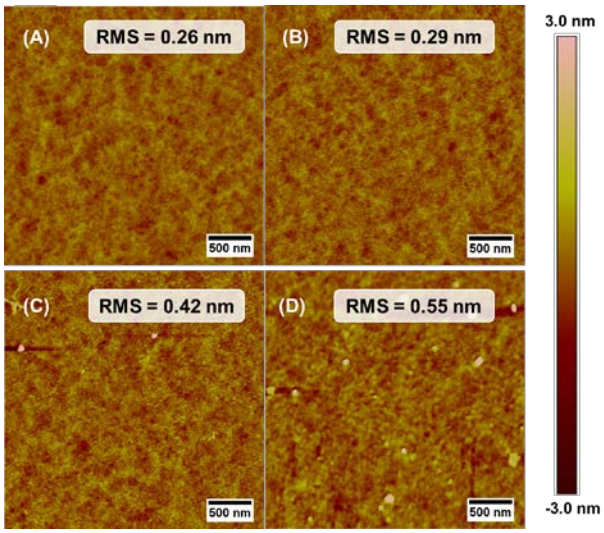

Figure 6: *AFM of (a) cleaned (b) Cl-terminated (c) functionalized with vac oven anneal and (d) post MLD and cap removal Ge.*

Active carrier concentration values from As-MLD doped Ge are shown in **Figure 7** where the RTA time was varied while maintaining a constant temperature of 650 °C. Using a conventional RTA system this is the maximum temperature permitted (~2/3 of melting temperature) for Ge as it has a melting point of 938.12 °C. The maximum carrier concentration for the first 8-10 nm shows values between 3×10^{19} and 4×10^{19} atoms/cm^3.

Surface artefacts are known to impact on the accuracy of the initial surface data point measured through ECV and lead to this data point often being disregarded when quoting maximum carrier concentrations. Maximum carrier concentration values after this surface point of > 1×10^{19} atoms/cm^3 represent the highest values seen to date with As-MLD. Previously, the maximum carrier concentration of As-MLD on Ge was approximately half of this at 6×10^{18} atoms/cm^3.[27] The solid solubility and maximum electrically active limits of arsenic in Ge have not been as widely reported on as the corresponding values for Si. Chui et al [49], reported that the maximum electrically active limit of As is 3.5×10^{19} atoms/cm^3 for Ge doped through implantation and activated with a 500°C RTA. Their study also noted that RTA temperatures above 600 °C lead to considerable As diffusion with a concurrent decrease in the maximum electrically active dopant levels to ~ 2×10^{19} atoms/cm^3. Other reports of As activation in Ge have placed the maximum activation level in a range between 1-3 $\times 10^{19}$ atoms/cm^3. [50-55] Duffy *et al* [56], have reported maximum activation limits in this 2×10^{19} atoms/cm^3 region for Ge doped with As through a gas phase source using RTA temperatures above 600 °C. Miyoshi *et al*, reported a maximum activation value with a form of microwave plasma doping at 4.3×10^{18} atoms/cm^3. [57] Analysis of the shape of the plots in **Figure 7** shows that they have box like profiles as have been seen in other As diffusion doping studies which are consistent with concentration enhanced diffusion.[58]

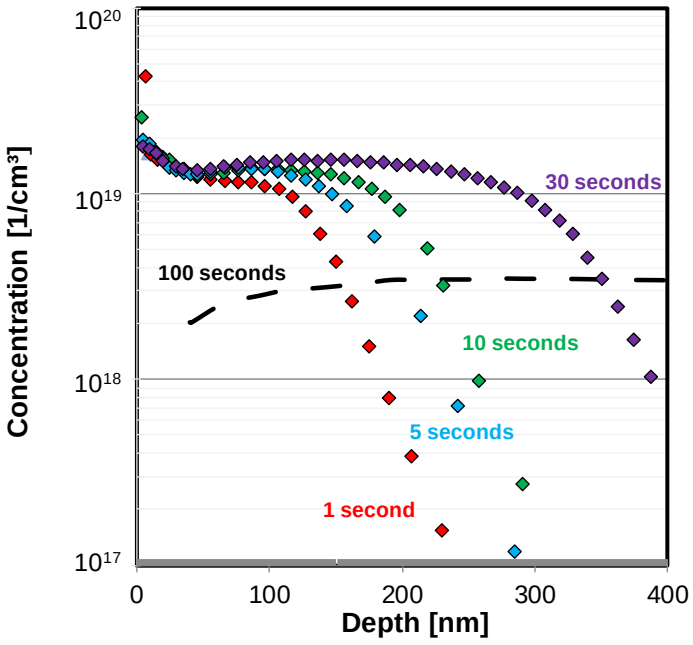

Figure 7: *ECV profiling of active carrier concentrations in Ge samples after arsenic MLD processing. RTA time has been varied with all samples receiving a 50 nm sputtered SiO_2 cap and 650 °C RTA*

Monolayer doping by nature is a limited source diffusion method of doping. Further indirect evidence of monolayer formation is provided through analysing the incorporated dose values from the ECV data. **Table 1** shows that dose values plateau at ~ 4×10^{14} atoms/cm^2. Profiles match the theory of limited source diffusion.[59] Between 30 seconds and 100 seconds the complete surface dose is incorporated and dopants which were situated close to the sample surface diffuse further into the bulk using a 100 second anneal.

Validation of the ECV data was attained from sheet resistance (Rs) measurements of the MLD doped blanket Ge samples. Through the formula outlined previously by Duffy *et al*, it was possible to translate carrier concentration profiles from ECV to a theoretical Rs value which was then compared to the experimentally determined value. [56] The correlation between the theoretical and experimentally measured Rs is shown in **Table 1** with reasonable agreement between the values, which corroborates the ECV data.

RTA time	**Dose (**atoms/cm^2**)**	**Sheet resistance (Ohm/sq)**	
		Theoretical (ECV)	**Measured value**
1 second	1.7×10^{14}	101	99
5 seconds	2.3×10^{14}	79	72
10 seconds	2.8×10^{14}	70	60
30 seconds	4.5×10^{14}	46	40
100 seconds	4.2×10^{14}	25	10

Table 1: *Total activated dose values in Ge from As-MLD with variations in RTA time using a 650 °C RTA. Sheet resistance values of selected samples were measured and compared to theoretical values to validate ECV data*

The pioneering work of Ho *et al* demonstrated the ability of MLD to provide controlled dopant doses to semiconductor materials, by the variation of dopant-containing molecule.[15] Since then, a number of studies have found success in controlling dose through MLD, such as those by Ye et al and Perego et al.[60] These studies have all focused on the application of phosphorus and boron MLD to silicon.

A rudimentary method of estimating the quantity of the arsanilic acid molecules which can pack onto the Ge surface, is to model the dimensions of the molecule, assume a spherical shape and calculate the maximum coverage on a semiconductor surface in a 2-dimensions (see **Figure 8**). Modelling work was carried out using Materials Studio© software. Triallylarsine (TAA) which was used for previous As-MLD studies on Ge has a

calculated diameter of 0.94 nm which translates to a theoretical "ideal" dose of ~ 1.5×10^{14} atoms/cm^2.[27, 34] Previous experimental work using TAA incorporated a maximum dose of 2×10^{14} atoms/cm^2. By comparison, arsanilic acid was calculated to have a diameter of 0.46 nm. An approximate maximum dose of ~ 6×10^{14} atoms/cm^2 was calculated from this 2-dimensional "ideal" packing scenario. Experimentally it was determined from ECV that an active dose of ~ 4×10^{14} atoms/cm^2 was incorporated. This corresponds with to approximately 70% of what could have been achieved with ideal packing. There are two reasons why 100% of the potential dose was not incorporated. The first being that the packing of the molecules was not ideal and spaces on the surface of Ge were present which were too small to incorporate a molecule, therefore full coverage was not achieved. The second is that some of the As from the molecules attached to the surface got trapped at the interface or in the capping layer. In reality it is probably a combination of both but a theoretical study to determine what the optimal packing could be for such molecules will be pursued in future studies. This provides an experimental validation of the theory, that changing size of the footprint of the dopant-containing molecule, between As-acid and TAA, allows for controlled adjustment of dose from 2×10^{14} atoms/cm^2 to 4×10^{14} atoms/cm^2. It is important to note that this approach for modulating dose, between As-acid and TAA, does require different monolayer reaction strategies. Further advancement of As-MLD on Ge by functionalisation with larger and smaller dopant-containing molecule sizes will allow for greater ability to tune the incorporated dose through MLD.

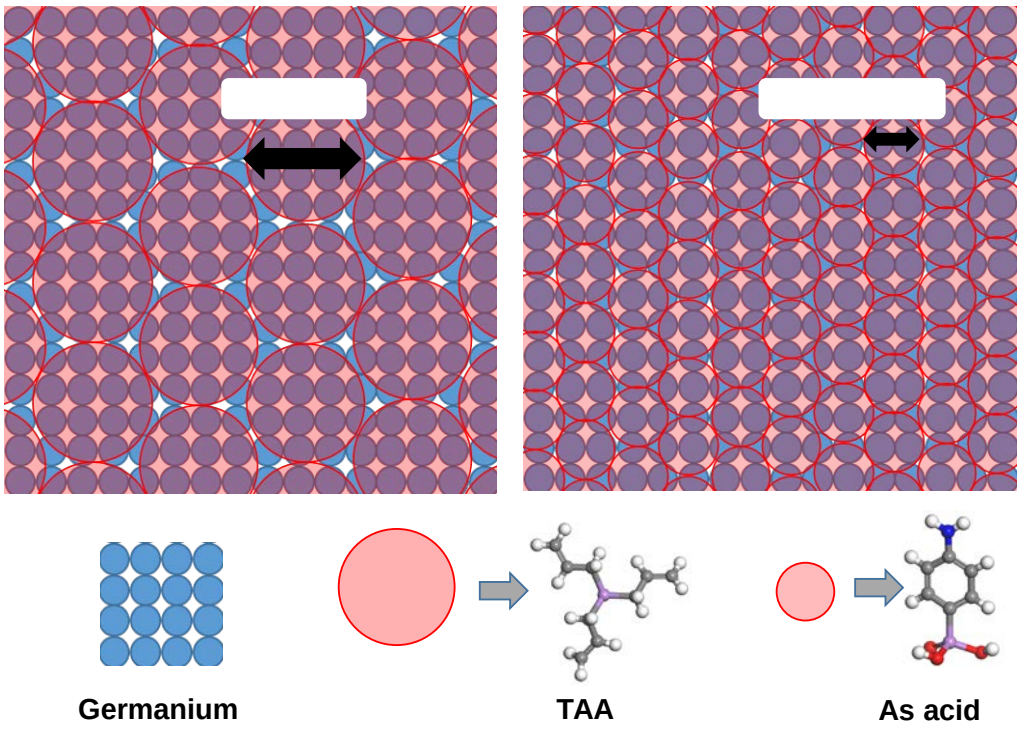

Figure 8: *2-dimensional depiction of packing density for arsenic MLD precursor arsanilic acid As acid) and a comparison with previously used triallylarsine (TAA)*

Dose values determined from ECV where the RTA temperature was varied (**Figure S3**) were used to calculate the diffusion co-efficient of arsenic introduced through MLD. These values are compared to previous literature where ECV was used. The methodology for calculating diffusion co-efficient has previously been outlined in the study of phosphorus doping of silicon-germanium. **Figure 9** demonstrates the increase in diffusion co-efficient with increasing RTA temperature. Our data shows some correlation with the previous As-MLD literature where triallylarsine was used as a dopant source.[27] Duffy et al, utilized a gas source (AsH_3) method for As diffusion and activation in Ge which shows lower diffusivity than results from arsanilic acid-MLD. [56] Temperature ramp rates of the annealing tools are likely to differ between each study, and the inclusion of additional elements such as carbon and nitrogen impacting diffusivity of As, may account for the difference in the diffusion co-efficient. All data sets have diffusion co-efficients which are in the extrinsic doping regime.

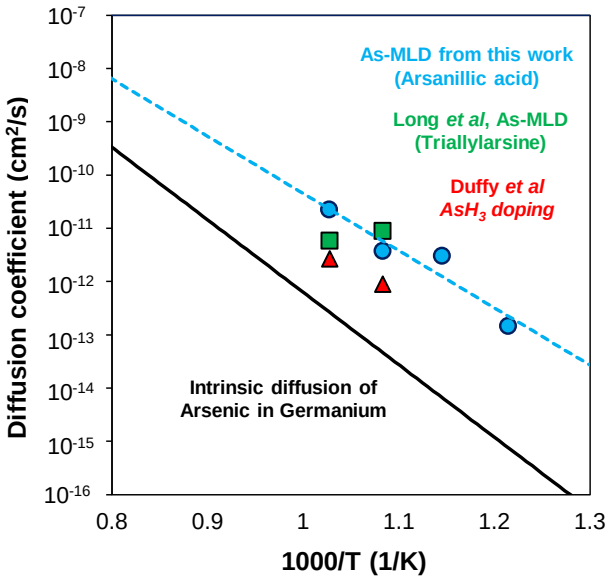

Figure 9: Diffusion co-efficient vs 1000/T, where T is in Kelvin. A black solid line is used to show intrinsic As diffusivity, red markers to show the previous work of Duffy *et al*, and blue markers to indicate As-MLD data from this work. Diffusion co-efficient from Duffy et al, and this work have been calculated from ECV.

With the aim of potential doping processes to decrease annealing temperatures, while maintaining or improving active carrier concentrations and minimizing diffusion depth, it is evident that MLD requires alternative methods of delivering dopant atoms into target substrates with reduced thermal budgets. Utilizing tools such as laser and

flash lamp annealing have shown promise for producing greater than solid solubility limit levels of dopants in Ge. [31, 61-63] Further studies into the combination of MLD with these advanced annealing techniques are important to demonstrate the true of potential of this doping methodology.

Conclusions

A new chemical route for functionalising Ge has offered the opportunity to controllably dope nanostructured Ge using As via monolayer doping, which overcomes many of the issues associated with ion implantation and permits a record As doping level to be achieved. It involves the functionalisation of Cl terminated Ge with a commercially available arsenic containing molecule, arsanilic acid. By applying this new chemical route we have demonstrated a simple, non-destructive approach for conformal doping of Ge producing n-type doping levels, rivalling beam-line implantation, which matches previously shown active solubility limits of arsenic (approx. 2×10^{19} atoms/cm^3) when using RTA temperatures greater than 600 °C. These active carrier concentrations are two times higher than what was the previously assumed limit of As-MLD on Ge and for the first time is at dopant levels that allow the use of Ge as the channel material in transistor devices. We demonstrate that anneal time allows control over the depth of diffusion of the arsenic dopants in Ge. By calculating the molecular footprint of the arsanilic acid and comparing it to that of triallylarsine used in a previous study we propose that the molecular footprint was be tuned (i.e. increasing or decreasing the size of the molecule) to control the dose of dopant that is delivered to Ge. Finally, the discovery of this new chemical functionalisation route significantly advances the field of surface functionalisation with implications for many potential applications and a broad range of materials.

References

1. Moore, G. E., Cramming more components onto integrated circuits (Reprinted from Electronics, pg 114-117, April 19, 1965). *Proceedings of the Ieee* **1998,** *86* (1), 82-85.
2. International Roadmap For Devices and Systems 2018 Update. IEEE.
3. Dayeh, S. A.; Chen, R.; Ro, Y. G.; Sim, J., Progress in doping semiconductor nanowires during growth. *Materials Science in Semiconductor Processing* **2017,** *62*, 135-155.
4. Gao, F.; Teplyakov, A. V., Challenges and opportunities in chemical functionalization of semiconductor surfaces. *Applied Surface Science* **2017,** *399*, 375-386.
5. Goley, P. S.; Hudait, M. K., Germanium Based Field-Effect Transistors: Challenges and Opportunities. *Materials* **2014,** *7* (3), 2301-2339.
6. Current, M.; Rubin, L. M.; Sinclair, F., Commercial Ion Implantation Systems. In *Ion Implantation Science and Technology- 2018*, Ion Implant Technology Co.: 2018; pp (03)2-41.
7. Duffy, R.; Van Dal, M. J. H.; Pawlak, B. J.; Kaiser, M.; Weemaes, R. G. R.; Degroote, B.; Kunnen, E.; Altamirano, E., Solid phase epitaxy versus random nucleation and growth in sub-20 nm wide fin field-effect transistors. *Applied Physics Letters* **2007,** *90* (24), 3.

8. Duffy, R.; Curatola, G.; Pawlak, B. J.; Doornbos, G.; van der Tak, K.; Breimer, P.; van Berkum, J. G. M.; Roozeboom, F., Doping fin field-effect transistor sidewalls: Impurity dose retention in silicon due to high angle incident ion implants and the impact on device performance. *Journal of Vacuum Science & Technology B* **2008,** *26* (1), 402-407.
9. Vandervorst, W.; Fleischmann, C.; Bogdanowicz, J.; Franquet, A.; Celano, U.; Paredis, K.; Budrevich, A., Dopant, composition and carrier profiling for 3D structures. *Materials Science in Semiconductor Processing* **2017,** *62*, 31-48.
10. Fair, R. B., History of some early developments in ion-implantation technology leading to silicon transistor manufacturing. *Proceedings of the Ieee* **1998,** *86* (1), 111-137.
11. Wood, B.; Khaja, F.; Colombeau, B.; Sun, S.; Waite, A.; Jin, M.; Chen, H.; Chan, O.; Thanigaivelan, T.; Pradhan, N.; Gossmann, H. J.; Sharma, S.; Chavva, V.; Cai, M. P.; Okazaki, M.; Munnangi, S.; Ni, C. N.; Suen, W.; Chang, C. P.; Mayur, A.; Variam, N.; Brand, A., Fin Doping by Hot Implant for 14nm FinFET Technology and Beyond. *Ulsi Process Integration 8* **2013,** *58* (9), 249-256.
12. Mizubayashi, W.; Onoda, H.; Nakashima, Y.; Ishikawa, Y.; Matsukawa, T.; Endo, K.; Liu, Y. X.; O'Uchi, S.; Tsukada, J.; Yamauchi, H.; Migita, S.; Morita, Y.; Ota, H.; Masahara, M.; Ieee, Heated Ion Implantation Technology for Highly Reliable Metal-gate/High-k CMOS SOI FinFETs. *2013 Ieee International Electron Devices Meeting (Iedm)* **2013**, 4.
13. Lee, J. W.; Sasaki, Y.; Cho, M. J.; Togo, M.; Boccardi, G.; Ritzenthaler, R.; Eneman, G.; Chiarella, T.; Brus, S.; Horiguchi, N.; Groeseneken, G.; Thean, A., Plasma doping and reduced crystalline damage for conformally doped fin field effect transistors. *Applied Physics Letters* **2013,** *102* (22), 4.
14. Qin, S.; Ieee, Plasma Doping (PLAD) for Advanced Memory Device Manufacturing. *2014 20th International Conference on Ion Implantation Technology (Iit 2014)* **2014**.
15. Ho, J. C.; Yerushalmi, R.; Jacobson, Z. A.; Fan, Z.; Alley, R. L.; Javey, A., Controlled nanoscale doping of semiconductors via molecular monolayers. *Nature Materials* **2008,** *7* (1), 62-67.
16. Kennedy, N.; Duffy, R.; Eaton, L.; O'Connell, D.; Monaghan, S.; Garvey, S.; Connolly, J.; Hatem, C.; Holmes, J. D.; Long, B., Phosphorus monolayer doping (MLD) of silicon on insulator (SOI) substrates. *Beilstein Journal of Nanotechnology* **2018,** *9*, 2106-2113.
17. Alphazan, T.; Mathey, L.; Schwarzwalder, M.; Lin, T. H.; Rossini, A. J.; Wischert, R.; Enyedi, V.; Fontaine, H.; Veillerot, M.; Lesage, A.; Emsley, L.; Veyre, L.; Martin, F.; Thieuleux, C.; Coperet, C., Monolayer Doping of Silicon through Grafting a Tailored Molecular Phosphorus Precursor onto Oxide-Passivated Silicon Surfaces. *Chemistry of Materials* **2016,** *28* (11), 3634-3640.
18. Arduca, E.; Mastromatteo, M.; De Salvador, D.; Seguini, G.; Lenardi, C.; Napolitani, E.; Perego, M., Synthesis and characterization of P delta-layer in SiO2 by monolayer doping. *Nanotechnology* **2016,** *27* (7), 5.
19. Hazut, O.; Agarwala, A.; Subramani, T.; Waichman, S.; Yerushalmi, R., Monolayer Contact Doping of Silicon Surfaces and Nanowires Using Organophosphorus Compounds. *Jove-Journal of Visualized Experiments* **2013,** (82), 5.
20. Ye, L.; Gonzalez-Campo, A.; Kudernac, T.; Nunez, R.; de Jong, M.; van der Wiel, W. G.; Huskens, J., Monolayer Contact Doping from a Silicon Oxide Source Substrate. *Langmuir* **2017,** *33* (15), 3635-3638.
21. Taheri, P.; Fahad, H. M.; Tosun, M.; Hettick, M.; Kiriya, D.; Chen, K.; Javey, A., Nanoscale Junction Formation by Gas-Phase Monolayer Doping. *Acs Applied Materials & Interfaces* **2017,** *9* (24), 20648-20655.
22. Hazut, O.; Yerushalmi, R., Direct Dopant Patterning by a Remote Monolayer Doping Enabled by a Monolayer Fragmentation Study. *Langmuir* **2017,** *33* (22), 5371-5377.
23. Veerbeek, J.; Ye, L.; Vijselaar, W.; Kudernac, T.; van der Wiel, W. G.; Huskens, J., Highly doped silicon nanowires by monolayer doping. *Nanoscale* **2017,** *9* (8), 2836-2844.
24. Kennedy, N.; Duffy, R.; Mirabelli, G.; Eaton, L.; Petkov, N.; Holmes, J. D.; Hatem, C.; Walsh, L.; Long, B., Monolayer doping of silicon-germanium alloys: A balancing act between phosphorus incorporation and strain relaxation. *Journal of Applied Physics* **2019,** *126* (2), 9.
25. Mattson, E. C.; Chabal, Y. J., Understanding Thermal Evolution and Monolayer Doping of Sulfur-Passivated GaAs(100). *Journal of Physical Chemistry C* **2018,** *122* (15), 8414-8422.
26. O'Connell, J.; Napolitani, E.; Impellizzeri, G.; Glynn, C.; McGlacken, G. P.; O'Dwyer, C.; Duffy, R.; Holmes, J. D., Liquid-Phase Monolayer Doping of InGaAs with Si-, S-, and Sn-Containing Organic Molecular Layers. *Acs Omega* **2017,** *2* (5), 1750-1759.
27. Long, B.; Verni, G. A.; O'Connell, J.; Shayesteh, M.; Gangnaik, A.; Georgiev, Y. M.; Carolan, P.; O'Connell, D.; Kuhn, K. J.; Clendenning, S. B.; Nagle, R.; Duffy, R.; Holmes, J. D., Doping top-down e-beam fabricated germanium nanowires using molecular monolayers. *Materials Science in Semiconductor Processing* **2017,** *62*, 196-200.
28. Sgarbossa, F.; Carturan, S. M.; De Salvador, D.; Rizzi, G. A.; Napolitani, E.; Maggioni, G.; Raniero, W.; Napoli, D. R.; Granozzi, G.; Carnera, A., Monolayer doping of germanium by phosphorus-containing molecules. *Nanotechnology* **2018,** *29* (46), 11.

29. Alphazan, T.; Alvarez, A. D.; Martin, F.; Grampeix, H.; Enyedi, V.; Martinez, E.; Rochat, N.; Veillerot, M.; Dewitte, M.; Nys, J. P.; Berthe, M.; Stievenard, D.; Thieuleux, C.; Grandidier, B., Shallow Heavily Doped n plus plus Germanium by Organo-Antimony Monolayer Doping. *Acs Applied Materials & Interfaces* **2017,** *9* (23), 20179-20187.
30. Brotzmann, S.; Bracht, H., Intrinsic and extrinsic diffusion of phosphorus, arsenic, and antimony in germanium. *Journal of Applied Physics* **2008,** *103* (3).
31. Sgarbossa, F.; Maggioni, G.; Rizzi, G. A.; Carturan, S. M.; Napolitani, E.; Raniero, W.; Carraro, C.; Bondino, F.; Pis, I.; De Salvador, D., Self-limiting Sb monolayer as a diffusion source for Ge doping. *Applied Surface Science* **2019,** *496*, 9.
32. Choi, K.; Buriak, J. M., Hydrogermylation of alkenes and alkynes on hydride-terminated Ge(100) surfaces. *Langmuir* **2000,** *16* (20), 7737-7741.
33. O'Connell, J.; Verni, G. A.; Gangnaik, A.; Shayesteh, M.; Long, B.; Georgiev, Y. M.; Petkov, N.; McGlacken, G. P.; Morris, M. A.; Duffy, R.; Holmes, J. D., Organo-arsenic Molecular Layers on Silicon for High-Density Doping. *Acs Applied Materials & Interfaces* **2015,** *7* (28), 15514-15521.
34. Long, B.; Verni, G. A.; O'Connell, J.; Holmes, J.; Shayesteh, M.; O'Connell, D.; Duffy, R.; Ieee, Molecular Layer Doping: Non-destructive Doping of Silicon and Germanium. *2014 20th International Conference on Ion Implantation Technology (Iit 2014)* **2014**, 4.
35. Longo, R. C.; Mattson, E. C.; Vega, A.; Cabrera, W.; Cho, K.; Chabal, Y. J.; Thissen, P., Mechanism of Arsenic Monolayer Doping of Oxide-Free Si(111). *Chemistry of Materials* **2016,** *28* (7), 1975-1979.
36. Longo, R. C.; Mattson, E. C.; Vega, A.; Cabrera, W.; Cho, K.; Chabal, Y.; Thissen, P., Atomic Mechanism of Arsenic Monolayer Doping on oxide-free Silicon(111). *Mrs Advances* **2016,** *1* (33), 2345-2353.
37. Peng, W. N.; Rupich, S. M.; Shafiq, N.; Gartstein, Y. N.; Malko, A. V.; Chabal, Y. J., Silicon Surface Modification and Characterization for Emergent Photovoltaic Applications Based on Energy Transfer. *Chemical Reviews* **2015,** *115* (23), 12764-12796.
38. Fabre, B., Functionalization of Oxide-Free Silicon Surfaces with Redox-Active Assemblies. *Chemical Reviews* **2016,** *116* (8), 4808-4849.
39. Sonawane, M. D.; Nimse, S. B., Surface Modification Chemistries of Materials Used in Diagnostic Platforms with Biomolecules. *Journal of Chemistry* **2016**.
40. Loscutoff, P. W.; Bent, S. F., Reactivity of the germanium surface: Chemical passivation and functionalization. In *Annual Review of Physical Chemistry*, Annual Reviews: Palo Alto, 2006; Vol. 57, pp 467-495.
41. Vega, A.; Thissen, P.; Chabal, Y. J., Environment-Controlled Tethering by Aggregation and Growth of Phosphonic Acid Monolayers on Silicon Oxide. *Langmuir* **2012,** *28* (21), 8046-8051.
42. Kresse, G.; Furthmuller, J., Efficient iterative schemes for ab initio total-energy calculations using a plane-wave basis set. *Physical Review B* **1996,** *54* (16), 11169-11186.
43. Kresse, G.; Joubert, D., From ultrasoft pseudopotentials to the projector augmented-wave method. *Physical Review B* **1999,** *59* (3), 1758-1775.
44. Blochl, P. E., PROJECTOR AUGMENTED-WAVE METHOD. *Physical Review B* **1994,** *50* (24), 17953-17979.
45. Perdew, J. P.; Wang, Y., ACCURATE AND SIMPLE ANALYTIC REPRESENTATION OF THE ELECTRON-GAS CORRELATION-ENERGY. *Physical Review B* **1992,** *45* (23), 13244-13249.
46. Kary, R. M.; Frisch, K. C., ARSONOSILOXANES. *Journal of the American Chemical Society* **1957,** *79* (9), 2140-2142.
47. Deiters, J. A.; Holmes, R. R., PATHWAYS FOR NUCLEOPHILIC-SUBSTITUTION AT SILICON - A MOLECULAR-ORBITAL APPROACH. *Journal of the American Chemical Society* **1987,** *109* (6), 1686-1692.
48. Sun, S. Y.; Sun, Y.; Liu, Z.; Lee, D. I.; Peterson, S.; Pianetta, P., Surface termination and roughness of Ge(100) cleaned by HF and HCl solutions. *Applied Physics Letters* **2006,** *88* (2).
49. Chui, C. O.; Kulig, L.; Moran, J.; Tsai, W.; Saraswat, K. C., Germanium n-type shallow junction activation dependences. *Applied Physics Letters* **2005,** *87* (9), 3.
50. Tsouroutas, P.; Tsoukalas, D.; Bracht, H., Experiments and simulation on diffusion and activation of codoped with arsenic and phosphorous germanium. *Journal of Applied Physics* **2010,** *108* (2).
51. Simoen, E.; Satta, A.; D'Amore, A.; Janssens, T.; Clarysse, T.; Martens, K.; De Jaeger, B.; Benedetti, A.; Hoflijk, I.; Brijs, B.; Meuris, M.; Vandervorst, W., Ion-implantation issues in the formation of shallow junctions in germanium. *Materials Science in Semiconductor Processing* **2006,** *9* (4-5), 634-639.
52. Satta, A.; Simoen, E.; Janssens, T.; Clarysse, T.; De Jaeger, B.; Benedetti, A.; Hoflijk, I.; Brijs, B.; Meuris, M.; Vandervorst, W., Shallow junction ion implantation in Ge and associated defect control. *Journal of the Electrochemical Society* **2006,** *153* (3), G229-G233.
53. Chui, C. O.; Gopalakrishnan, K.; Griffin, P. B.; Plummer, J. D.; Saraswat, K. C., Activation and diffusion studies of ion-implanted p and n dopants in germanium. *Applied Physics Letters* **2003,** *83* (16), 3275-3277.

54. Koffel, S.; Kaiser, R. J.; Bauer, A. J.; Amon, B.; Pichler, P.; Lorenz, J.; Frey, L.; Scheiblin, P.; Mazzocchi, V.; Barnes, J. P.; Claverie, A., Experiments and simulation of the diffusion and activation of the n-type dopants P, As, and Sb implanted into germanium. *Microelectronic Engineering* **2011,** *88* (4), 458-461.
55. Prussing, J. K.; Hamdana, G.; Bougeard, D.; Peiner, E.; Bracht, H., Quantitative scanning spreading resistance microscopy on n-type dopant diffusion profiles in germanium and the origin of dopant deactivation. *Journal of Applied Physics* **2019,** *125* (8).
56. Duffy, R.; Shayesteh, M.; Thomas, K.; Pelucchi, E.; Yu, R.; Gangnaik, A.; Georgiev, Y. M.; Carolan, P.; Petkov, N.; Long, B.; Holmes, J. D., Access resistance reduction in Ge nanowires and substrates based on non-destructive gas-source dopant in-diffusion. *Journal of Materials Chemistry C* **2014,** *2* (43), 9248-9257.
57. Miyoshi, H.; Oka, M.; Ueda, H.; Ventzek, P. L. G.; Sugimoto, Y.; Kobayashi, Y.; Nakamura, G.; Hirota, Y.; Kaitsuka, T.; Kawakami, S., Microwave plasma doping: Arsenic activation and transport in germanium and silicon. *Japanese Journal of Applied Physics* **2016,** *55* (4).
58. Larsen, A. N.; Larsen, K. K.; Andersen, P. E.; Svensson, B. G., HEAVY DOPING EFFECTS IN THE DIFFUSION OF GROUP-IV AND GROUP-V IMPURITIES IN SILICON. *Journal of Applied Physics* **1993,** *73* (2), 691-698.
59. Kadhim, M. A. H.; Tuck, B., ON SOLID-STATE DIFFUSION FROM A LIMITED SOURCE. *Physica Status Solidi a-Applied Research* **1980,** *58* (1), 303-310.
60. Ye, L.; Pujari, S. P.; Zuilhof, H.; Kudernac, T.; de Jong, M. P.; van der Wiel, W. G.; Huskens, J., Controlling the Dopant Dose in Silicon by Mixed-Monolayer Doping. *Acs Applied Materials & Interfaces* **2015,** *7* (5), 3231-3236.
61. Milazzo, R.; Napolitani, E.; Impellizzeri, G.; Fisicaro, G.; Boninelli, S.; Cuscuna, M.; De Salvador, D.; Mastromatteo, M.; Italia, M.; La Magna, A.; Fortunato, G.; Priolo, F.; Privitera, V.; Carnera, A., N-type doping of Ge by As implantation and excimer laser annealing. *Journal of Applied Physics* **2014,** *115* (5), 5.
62. Boninelli, S.; Milazzo, R.; Carles, R.; Houdellier, F.; Duffy, R.; Huet, K.; La Magna, A.; Napolitani, E.; Cristiano, F., Nanoscale measurements of phosphorous-induced lattice expansion in nanosecond laser annealed germanium. *Apl Materials* **2018,** *6* (5).
63. Hellings, G.; Rosseel, E.; Simoen, E.; Radisic, D.; Petersen, D. H.; Hansen, O.; Nielsen, P. F.; Zschatzsch, G.; Nazir, A.; Clarysse, T.; Vandervorst, W.; Hoffmann, T. Y.; De Meyer, K., Ultra Shallow Arsenic Junctions in Germanium Formed by Millisecond Laser Annealing. *Electrochemical and Solid State Letters* **2011,** *14* (1), II39-II41.

Table of Contents graphic only.